Advances in Environmental Technology 4 (2020) 175-185

Iranian Reasearch Organization for Science and Technology (IROST)

Advances in Environmental Technology

Journal home page: https://aet.irost.ir/

Reusability, optimization, and adsorption studies of modified graphene oxide in the removal of Direct Red 81 using response surface methodology

Avideh Azizi[1], Elham Moniri[2,*], Amir Hessam Hassani[1], Homayon Ahmad Panahi[3]

[1] *Department of Environmental Engineering, Faculty of Natural Resources and Environment, Science and Research Branch, Islamic Azad University, Tehran, Iran*

[2] *Department of Chemistry, Varain (Pishva) Branch, Islamic Azad University, Pishva, Iran*

[3] *Department of Chemistry, Central Tehran Branch, Islamic Azad University, Tehran, Iran*

ARTICLE INFO

Article history:
Received 23 September 2020
Received in revised form
10 June 2021
Accepted 18 June 2021

Keywords:
Direct Red 81
Graphene oxide
Regeneration
Response surface methodology Optimization

ABSTRACT

In the present study, graphene oxide (GO) was synthesized by the oxidation of graphite powder using the Hummers method. The GO was polymerized with poly methyl vinyl ketone (PMVK) and aniline (GO-MVK-ANI). It was utilized as the effective adsorbent towards the removal of Direct Red 81 (DR 81) in aqueous solutions. Response surface methodology (RSM) was applied for optimization and adsorption studies of Direct Red 81 removal using GO-MVK-ANI. According to the RSM results, the effects of the main parameters (the adsorbent dose, contact time, and pH) in dye removal efficiency were investigated. The R^2 value of 99.99% indicated that the predictions of the RSM model were acceptable for Direct Red 81 adsorption onto the adsorbent. The regeneration of GO-MVK-ANI for the dye adsorption showed fine efficacy in up to seven times of recyclability. The RSM model was used to evaluate the respective minimum and maximum values of 56.52% and 99.90% for the removal efficiencies of Direct Red 81.

1. Introduction

Dye-contaminated water is an important challenge facing many industries such as paper printing, textile, cosmetics, leather, and plastics due to the careless disposal of dye [1,2]. Among these dyes, azo-based dyes are one of the most typically applied synthetic dyes and are a carcinogenic and mutagenic hazard [3]. Direct Red 81, which is azo-based, contains a variety of toxic compounds [4]. Furthermore, the structure of azo dyes includes aromatic rings [5]. Hence, an efficient method should be applied for the removal of these dyes from industrial wastewater. The dye wastewaters can be treated via widely-used techniques that involve filtration, adsorption, ion exchange, chemical oxidation, membrane separation, coagulation, electrolysis, and biological treatment [5-7]. Among these, adsorption is considered one of the most applied processes by reason of its low cost, no secondary pollution, high efficiency, robustness, easy design, simple operation,

*Corresponding author. Tel: 0098-91-2501-1003
E-mail: moniri30003000@yahoo.com
DOI: 10.22104/AET.2021.4347.1239

environmentally friendly, and available adsorbents [8-12]. In recent years, a number of adsorbents have been utilized for dye adsorption from aqueous environments: clay, active carbon, carbon nanotube, fly ash, molecular sieves, graphene oxide (GO), perlite, cellulose, and zeolites [3,6,8]. A new fascinating material for the removal of various contaminants from wastewater is GO with a number of hydroxyl, carboxyl, and epoxy groups [6,13]. Actually, GO is the oxidized structure of graphene containing oxygen functional groups. These functional groups exist on GO and cause the following four phenomena [3,6]: (1) GO is modifiable; (2) when this adsorbent is dispersed in water, the solution is stable and homogenous; (3) high interactions with organic dyes; (4) and GO is more reactive than graphite. Meanwhile, graphene can be marked as an effective adsorbent because of its low cost, recycling with insignificant changes in its adsorption capacity, and environmental friendliness [14]. If the graphene is modified or polymerized, its application can be increased [14]. Some studies report good adsorption performance with GO based materials for Direct Red 81 removal [15,16].The present work aims to obtain and report the results of the Direct Red 81 adsorption behavior of polymerized GO via PMVK and aniline using RSM. Three experimental controlling parameters (adsorbent dose, contact time, and initial pH) were investigated for dye adsorption from aqueous solutions. Finally, the optimum conditions were identified for dye removal, and the adsorbent was reused for seven cycles under these conditions.

2. Materials and methods

2.1. Materials

All materials used in the research are presented in Table 1.

2.2. Synthesis of GO

GO was synthesized based on the Hummers and Offeman method [17]. The GO was prepared by adding 10 g of graphite powder to 230 mL H_2SO_4 in a 5 L beaker; then 5 g of $NaNO_3$ and 30 g of potassium persulfate were added to the mixture. The mixture was stirred by a magnetic stirrer for 2 h in an ice-water bath. In the next step, 460 mL of distilled water was slowly added to the reaction under constant stirring. Then, 325 mL of H_2O_2 (30%) was added to the solution, and the reaction was allowed to proceed at 90–100°C for about 2 h until the formation of a greenish-yellow color. After synthesis, the solid in suspension was washed with HCl (3%) and distilled water until the pH was 7. Finally, the product was maintained in an oven at 40°C for 3 days. The characteristics of the sample were studied using Fourier transform-infrared resonance (FTIR), Brunauer-Emmett-Teller (BET), energy-dispersive X-ray (EDX) spectroscopy, and scanning electron microscopy (SEM).

Table 1. Characteristic of materials.

Material	Characteristic	Company Name
Graphite powder	particle size < 50 μ m, purity ≥ 99.5%	Merck
Potassium persulfate	-	Merck
$NaNO_3$	-	Merck
H_2SO_4	95%-97%	Merck
H_2O_2	30%	Merck
HCl	37%	Merck
Ammonium persulfate	-	Merck
Dimethylformamide	purity ≥ 99.8%	Merck
Methanol	purity ≥ 99.5%	Merck
Allylamine	-	Fluka
Ethanol	purity ≥ 99.5%	Merck
Methyl vinyl ketone	-	Sigma-Aldrich
Aniline	-	Merck
Direct Red 81		Sigma-Aldrich

2.3. Synthesis of GO-MVK-ANI

The GO-MVK-ANI was prepared by a three-step procedure based on the report of [14]. First, 20 mL of dimethylformamide and 2 g of GO were added to a flask under stirring until the GO dissolved. Next, 10 mL of allylamine was added to the mixture and stirred at 160 rpm for 2 days. Then the final mixture was collected after washing with dimethyl-formamide and drying at room temperature. The grafting of the GO with allylamine (GO-AA) was dispersed in 30 mL of methanol. In the next step, 0.75 g ammonium persulfate (APS) initiator, 30 mL methyl vinyl ketone, and the dissolved GO-AA in methanol were added to the flask. The mixture was refluxed at 60 °C for 5 h in a nitrogen atmosphere with continuous stirring. The product was washed

with methanol, and after filtering, the adsorbent was dried at room temperature. In the final step, the prepared adsorbent was dispersed in 150 mL of ethanol, and then 50 mL of aniline was added to the mixed solution. The mixture was fixed under the condenser system with the atmosphere of nitrogen at 40°C for 6 h under stirring (180 rpm). Next, the product was filtered and washed with ethanol. The final adsorbent was left in the vacuum oven at 40°C for 3 days. The GO-MVK-ANI was measured by FTIR, BET, EDX, and SEM analyses.

2.4. Dye sorption

The batch experiments were carried out in a 50 mL glass flask for Direct Red 81 removing from aqueous environments. The initial dye concentration in each sample was 20 mg/L. The solutions were left in the rotary shaker (IKA, KS 260 Basic, Korea). After stirring at 150 rpm, the solutions were filtered using a syringe filter. The Direct Red 81 concentration was quantified by using a HACH spectrophotometer (DR 5000) at the wavelength corresponding to the maximum absorbance of 509 nm (λ_{max}). The extent of the adsorbent capacity and removal efficiency of dye was measured according to the following equations:

$$q_t = \frac{(C_0 - C_t)v}{m} \quad (1)$$

$$RE(\%) = \left(\frac{C_0 - C_t}{C_0}\right)100 \quad (2)$$

where q_t is the adsorbent capacity of dye (mg/g), RE is the dye removal efficiency, C_0 is the initial dye concentration (mg/L), C_t is the dye concentration at t time (mg/L), m is the mass of adsorbent (g), and v is the volume of the solution (L).

2.5. Regeneration test

Graphene-based materials could be effectively regenerated and reused. Therefore, regeneration studies of the adsorbent were carried out several times under optimum conditions via washing with methanol and distilled water. The samples were filtered and centrifuged for 5 min at 3000 rpm and then analyzed with a spectrophotometer.

2.6. Experimental design

One of the most important optimization processes in experimental studies is RSM based on a central composite design (CCD). RSM can be used for modeling, design of experiments, optimizing and analyzing of the connection between the factors [18,19]. The parameters of adsorbent dose, contact time, and initial pH were analyzed with a standard CCD. The number of tests for the three main factors included the standard 2^3 factorial points, consisting of 8 factorial points, 6 axial points, and 6 replicates at the center points. The test numbers were calculated according to Equation 3 [18]:

$$N = 2^n + 2n + n_c = 2^3 + (2 \times 3) + 6 = 20 \quad (3)$$

where N is the total number of experiments required.

The levels of the selected variables according to RSM design are listed in Table 2.

Each independent variable was coded in five levels (-1.68179, -1, 0, 1 and 1.68179) by the following equation [20]:

$$x_i = \frac{(X_i - X_0)}{\delta X} \quad (4)$$

where x_i is the coded value, X_i is the real value, X_0 is the real value of X_i at center point, and δX indicates the stage change.

Table 2. Experimental independent variables and their coded levels.

Variable	Symbol	Levels of coded variables				
		-α	Low	Medium	High	+α
		-1.68179	-1	0	1	1.68179
Adsorbent dose (g/L)	X_1	0.220	0.8	1.65	2.5	3.079
Contact time (min)	X_2	10.91	45	95	145	179.09
Initial pH	X_3	4.32	5	6	7	7.68

The quadratic equation model is expressed by the following equation [18]:

$$Y_i = b_0 + \sum_{i=1}^{n} b_i x_i + \sum_{i=1}^{n} b_{ii} x_i^2 + \sum_{i=1}^{n-1} \sum_{j=i+1}^{n} b_{ij} x_i x_j \quad (5)$$

where Y is the predicted response (Direct Red 81 removal efficiency), b_0 and b_i are the constant and linear coefficients, b_{ii} is the quadratic coefficient, b_{ij} is the interaction coefficient, and x_i and x_j present the coded values of the parameters. The

experiment for the removal of Direct Red 81 by GO-MVK-ANI was designed using MINITAB software, version 16. The validity of the models was explained by the analysis of variance method (ANOVA) with a 95% confidence level and the coefficient of R^2. Also, the predicted optimum condition was applied for the maximum dye removal efficiency in the optimization process.

3. Results and discussion

3.1. Characterization of adsorbent

The results of the FTIR (Thermo Nicolet, model: NEXUS 870 FT-IR, USA) spectrum of GO (Figure 1a) reveal the presence of peaks at 1054 and 1222 cm^{-1}, which are due to the C–O groups [13]. The bands at 1421 and 1720 cm^{-1} are attributed respectively to the CH_2 and C=O groups; the bending vibrations corresponding to O-H stretching are observed at 1628 and 3440 cm^{-1} [13,21] A band at 2922 cm^{-1} indicates the presence of an aliphatic C–H peak [22]. The spectrum of GO-MVK-ANI (Figure 1b) displays several bands, which represents the following groups: 1083 cm^{-1} (C–O groups), 1415 cm^{-1} (C=N stretching vibration), 1587 cm^{-1} (C=C aromatic groups), 1723 cm^{-1} (C=O groups), 3030 cm^{-1} (C–H aromatic), and 3225 cm^{-1} (O-H and N-H groups) [14]. The total pore volume and average pore diameter were determined according to N_2 adsorption-desorption isotherms at 77 K by a BET analyzer (BELSORP-mini II, Japan). The total pore volume was calculated with the adsorbed amount at a relative pressure (P/P0) of 0.990. In addition, the average pore diameter and total pore volume of the product were evaluated using the Barrett–Joyner-Halenda (BJH) technique. After the polymerization and modification process, the average pore diameter and total pore volume of the GO increased from 4.853 to 23.187 nm and from 0.016 to 0.022 cm^3/g, respectively [14]. The enhancement in the pore size can be attributed to the linked chain of functional groups to GO layers, which may be the result of higher space. The chemical analysis of the adsorbent was performed by using the EDX detector (Oxford instruments) attached to a field emission scanning electron microscope (FESEM, Zeiss, model: Sigma, Germany). The EDX result provides evidence for the presence of carbon (52.43%) and oxygen (47.57%) in the GO. For GO-MVK-ANI, the elemental composition of the adsorbent was changed to carbon (43.33%), oxygen (51.71%), and nitrogen (4.96%) after modification [14]. Also, the existence of nitrogen in GO-MVK-ANI is a reason for the successful preparation of the final adsorbent. FESEM analysis was carried out to observe the morphologies and microstructures of the adsorbent images. They can be seen from FESEM images in Figure 2. The SEM photographs of the adsorbents show that the whole sheets have crumples and folds. Furthermore, these wrinkles can be the reason why the sheets are flexible. The cause of this crumple can be ascribed to the abundant oxygen-containing functional groups on the surface of GO. The surface morphology photos demonstrate that the GO-MVK-ANI sheets are more lamellar than those of GO. Because the Π-Π stacking can increase the layer in adsorbent structure. Also, the surface on GO-MVK-ANI is more uneven than GO that this unevenness may be related to polymer chains [6].

3.2. Effect of main parameters on the adsorption

The effect of three main parameters (the adsorbent dose, contact time and initial pH) on the removal of Direct Red 81 by GO-MVK-ANI are displayed in Figure 3.

The effect of the adsorbent dose on the Direct Red 81 removal percentage is shown in Fig. 3a. It can be noticed that the removal percentage improves rapidly with the increase in the adsorbent dose. Similar results have been reported by other researchers [4,14,20]. The increase in the adsorption percentage is due to the adsorbent surface area and availability of more active adsorption sites on the GO-MVK-ANI surface at a higher adsorbent dose [20]. On the other hand, by enhancing the adsorbent dose, the active functional groups increase [14].

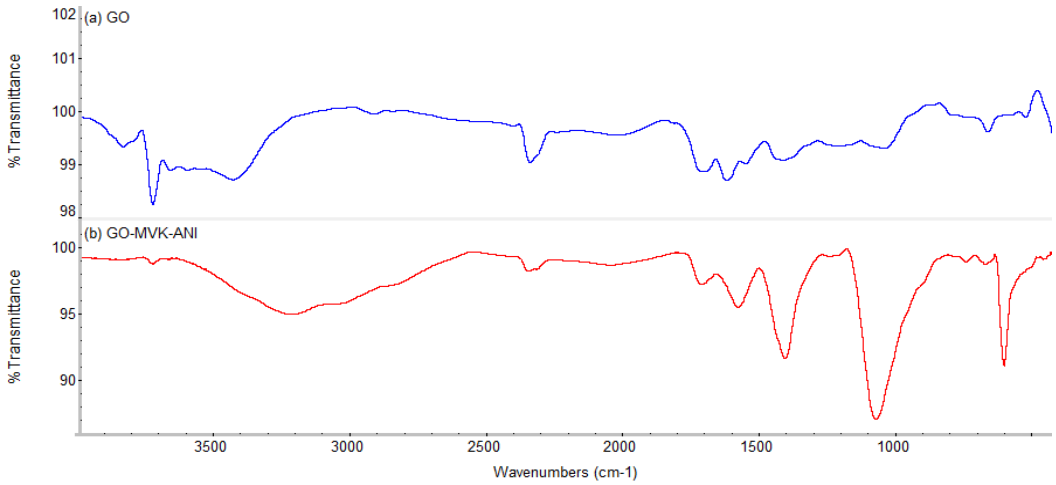

Fig. 1. FTIR spectra of (a) GO and (b) GO-MVK-ANI.

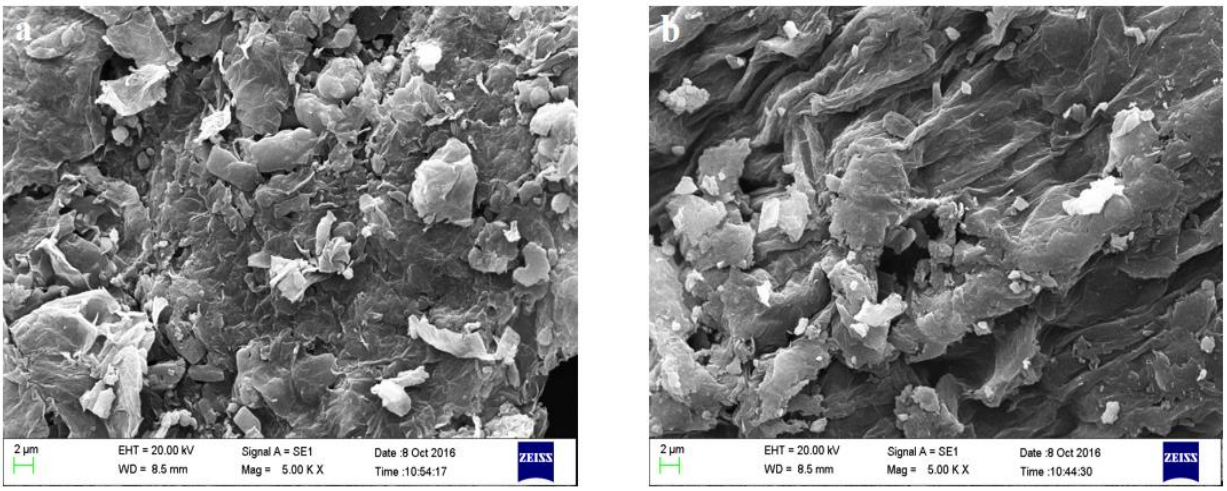

Fig. 2. SEM images of adsorbents (a) GO and (b) GO-MVK-ANI.

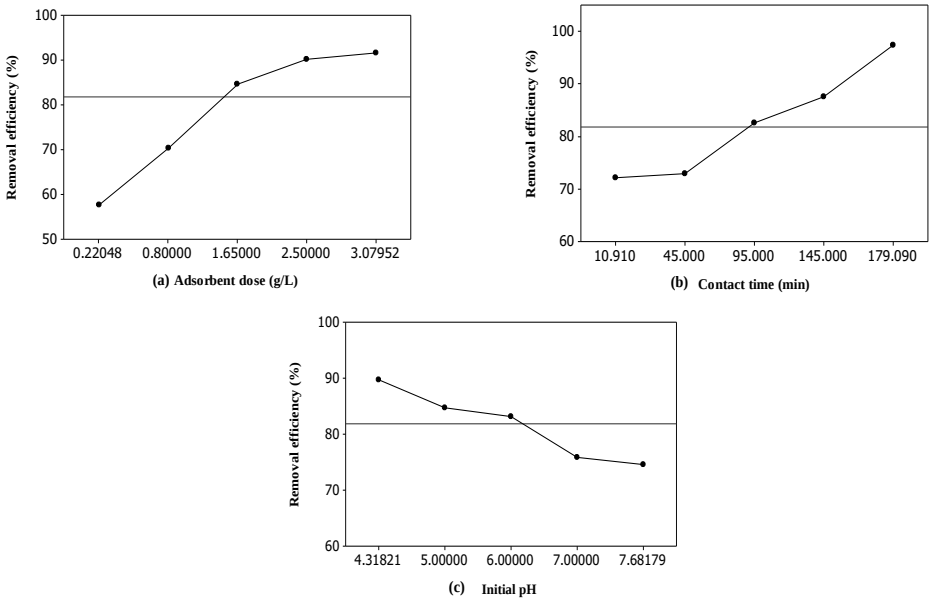

Fig. 3. Main effects of (a) adsorbent dose, (b) contact time and (c) initial pH on dye removal efficiency using GO-MVK-ANI.

The result of the time-dependent experiment is displayed in Figure 3b. The removal of Direct Red 81 by adsorption on the GO-MVK-ANI increases with time and attains a maximum removal efficiency (98%) at about 180 min. The accessibility of more active sites can be responsible for faster adsorption upto180 min [14,23]. The effect of initial pH on dye concentration is illustrated in Fig. 3c. The results show that the adsorption percentage decreases with an increase of pH value from 4.32 to 7.68. Direct Red 81 (anionic dye) includes the sulfonic acid groups, which can be protonated to the neutral form (R-SO_3H), at acidic pH. Moreover, the sulfonic groups display a negative charge at higher acidic solutions. The surface of GO has functional oxygen groups, including carboxylic groups (-COOH) and hydroxylic groups (-OH). At an acidic pH, carboxylic and hydroxylic groups are protonated to the cationic form. Consequently, the reason for the high adsorption capacity at a pH of 4.32 can be due to the electrostatic force of attraction between negatively charged dye molecules and positively charged functional oxygen groups [3]. The higher adsorption of anionic dye via carbon-based adsorbent at acidic pH is supported by the data reported in other researches [3,24,25].

3.3 *Comparison* of different adsorbents for the adsorption of Direct Red

The maximum adsorption capacity of GO-MVK-ANI for Direct Red 81 removal was 11.8 mg/g for an adsorbent dose of 1.65 g/L, contact time of 180 min, and pH of 6. The adsorption capacities for Direct Red comparing different adsorbent materials are summarized in Table 3. The contact time of adsorption for mixture almond shells and soy meal hull is 300 min and 24 h, respectively. Whereas, the equilibrium contact time of GO-MVK-ANI is obtained at 100 min. The prepared adsorbent demonstrates suitable adsorption ability for dye. Consequently, GO-MVK-ANI is an outstanding element of GO-based adsorbents.

3.4 RSM modeling

In this study, the central composite design matrix is given in Table 4, which shows the design of experiments together with the experimental results. Low P values for adsorbent dose (x_1), contact time (x_2), initial pH (x_3), all quadratic terms, and all interactive terms (P = 0.000 for all except x_{22} and x_1x_3 (P values of 0.001 and 0.267, respectively)) confirm the high significance of these parameters in this response.

The final model for Direct Red 81 removal efficiency is expressed by Equation 6:

$$\begin{aligned} Y = {} & 85.4125 + 10.0149x_1 + 7.3590x_2 \\ & - 4.4617x_3 - 3.7949{x_1}^2 \\ & - 0.2099{x_2}^2 - 1.1663{x_3}^2 \\ & -1.4438x_1x_2 - 0.0713x_1x_3 + 0.6687x_2x_3 \end{aligned} \quad (6)$$

The ANOVA for the model explains the adequacy of the model. The R^2 value, predicted R^2 value, and adjusted R^2 value were 99.99%, 99.93% and 99.98%, respectively, which were near to 1. The high R^2 values show that the accuracy of the RSM model is acceptable. Additionally, the polynomial model is in agreement with the experimental data based on the high adjusted R^2 value. The residual plots were analyzed for investigating the model adequacy and are shown in Figure 4a-c. The normal probability plot is used for judging the normality of the residuals. As shown in Figure 4a, the residuals near to a straight line indicate that they are normally spread in the model response. The plot in Figure 4b reveals that the model is reliable. The predicted values against the experimental values for the Direct Red 81 removal are illustrated in Figure 4c. The predicted values are close to the actual values. This result confirms that the model is successful. Ultimately, the 3D plots including the effect of adsorbent dose, contact time, and initial pH on dye removal efficiency by GO-MVK-ANI are presented in Figure 5. This figure shows that the reaction of these three parameters approximately had the same effect on Direct Red 81 adsorption. RSM was also applied in order to optimize the main variables in Direct Red 81 removal based on the target of 90%. Under the optimum condition predicted by the model (the adsorbent dose of 1.64 g/L, contact time of 100 min, and pH of 4.32), the dye removal efficiency was 89%. Therefore, it was concluded that the experimental value was close to the target value.

3.5. Regeneration process

The regeneration process is economic and reasonable for the pollutant-loaded adsorbent. The adsorbent was regenerated under optimum conditions (the contact time of 100 min, pH of 4.32, and adsorbent dose of 1.64 g/L). This stage was repeated seven times, and the regenerated GO-

MVK-ANI was washed with methanol and distilled water for every cycle. The results are presented in Fig. 6. After the first and second use, the removal efficiency reached 86.57%. Then, the efficiency of the adsorbent for Direct Red 81 removal after three times decreases from 86.57% to 80.3%. The adsorption percentage remained almost constant, but it decreased from 80.3% to 70.34% in the seventh cycle. Similar results have been reported for the regeneration of graphene-based adsorbent[13,30,31]. Many studies describe fine recycling behavior by graphene and GO based materials [32]. In this process, the suitable removal efficiency may be due to the considerable number of active sites recovered after washing.

Table 3. Maximum adsorption capacities of various adsorbents towards Direct Red

Adsorbent	Dye	Adsorption capacity (mg/g)	Ref
GO	Direct Red 23	15.3	[3]
Orange peel	Direct Red 23	10.718	[26]
Polyurethane foam (PUF)	Direct Red 80	4.50	[27]
Mixture almond shells	Direct Red 80	22.422	[28]
Soy meal hull	Direct Red 81	120.48	[29]
GO-MVK-ANI	Direct Red 81	11.8	The present study

Table 4. Observed and predicted results of experiments corresponding to RSM design.

Run order	Adsorbent dose (x_1)	Contact time (x_2)	Initial pH (x_3)	Dye removal efficiency (%)	
				Observed	Predicted
1	0.00000	-1.68179	0.00000	72.22	72.44
2	-1.00000	-1.00000	1.00000	56.52	56.36
3	-1.00000	1.00000	-1.00000	82.65	82.75
4	0.00000	0.00000	0.00000	85.57	85.41
5	0.00000	1.68179	0.00000	97.39	97.19
6	1.68179	0.00000	0.00000	91.60	91.52
7	0.00000	0.00000	0.00000	85.37	85.41
8	-1.68179	0.00000	0.00000	57.73	57.83
9	0.00000	0.00000	0.00000	85.37	85.41
10	-1.00000	-1.00000	-1.00000	66.60	66.48
11	1.00000	1.00000	-1.00000	99.90	100.00
12	0.00000	0.00000	-1.68179	89.70	89.61
13	1.00000	-1.00000	1.00000	79.26	79.13
14	1.00000	1.00000	1.00000	92.21	92.30
15	0.00000	0.00000	1.68179	74.50	74.61
16	1.00000	-1.00000	-1.00000	89.54	89.54
17	0.00000	0.00000	0.00000	85.30	85.41
18	0.00000	0.00000	0.00000	85.30	85.41
19	0.00000	0.00000	0.00000	85.57	85.41
20	-1.00000	1.00000	1.00000	75.33	75.30

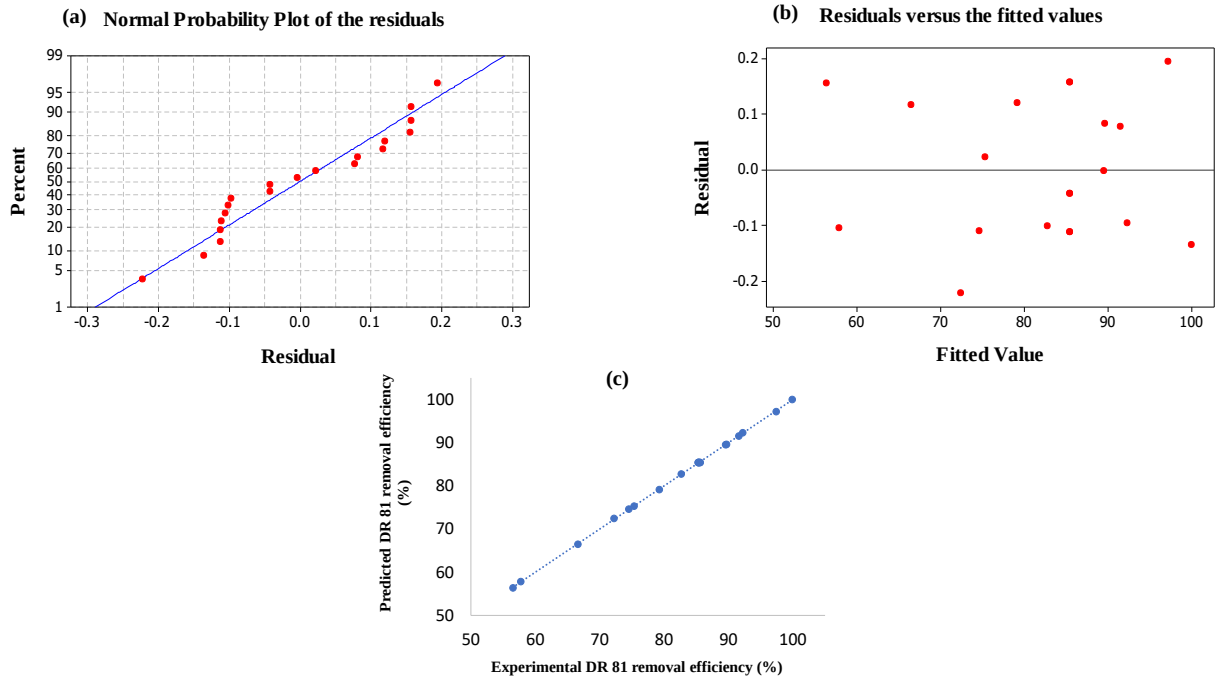

Fig. 4. (a) and (b) Normal probability and residual versus fit plots for Direct Red 81 removal efficiency; (c) Actual and predicted plot of adsorption of Direct Red 81.

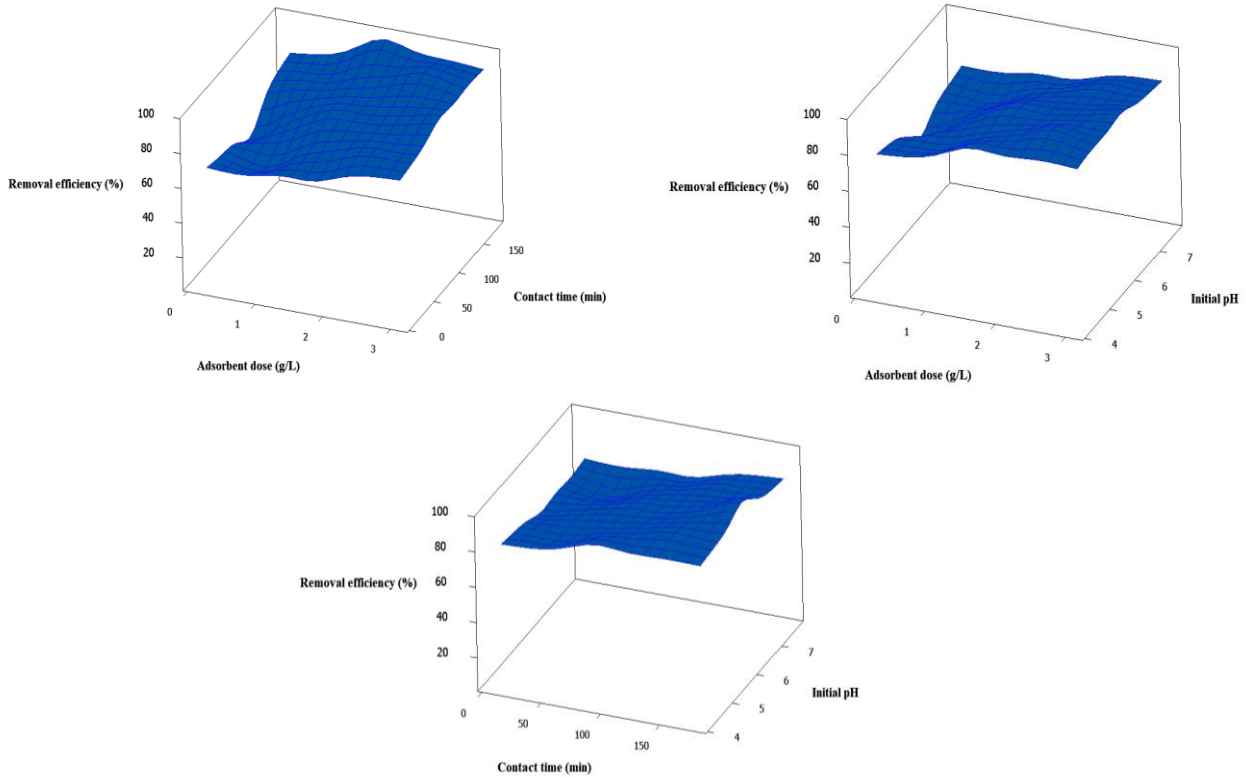

Fig. 5. Three dimensions surface plots of the parameters effect in Direct Red 81 removal efficiency.

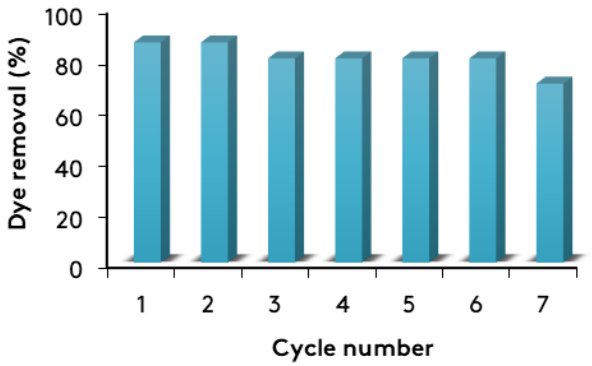

Fig. 6. Reuse of GO-MVK-ANI in Direct Red 81 removal under conditions: (initial dye concentration: 20 mg/L; adsorbent dose: 1.64 g/L; contact time: 100 min; pH: 4.32; room temperature: 23°C, shaker speed: 150 rpm).

4. Conclusions

The modified GO was synthesized and used as an effective adsorbent for the removal of Direct Red 81 from aqueous solutions via RSM. After the modification of GO, its average pore diameter increased from 4.853 to 23.187 nm. The suitability of the selected model was proven with the high R^2 value (99.99%), predicted R^2 value (99.93%), and adjusted R^2 value (99.98%); the predicted statistical values were also close to the experimental values. The optimum operating conditions for Direct Red 81 adsorption were the adsorbent dose of 1.64 g/L, contact time of 100 min, and pH of 4.32. The experiment was tested in optimized conditions for a target of 90%, and the result of dye removal efficiency was 89%. Moreover, the results showed that the adsorption at the equilibrium of Direct Red 81 was favorable at an acidic pH. Finally, the regeneration results indicated a removal efficiency of more than 70%, even after seven cycles. Therefore, it can be suggested that GO-MVK-ANI is a reusable adsorbent that can be repeatedly used for dye adsorption with a negligible drop in its removal efficiency.

Acknowledgement

We are grateful to the Science and Research Branch, Islamic Azad University (SRBIAU). In addition, the authors would like to express their gratitude to Mrs. Armineh Azizi (Postdoctoral Research Fellow of Ryerson University) for her consultations during the experiments.

References

[1] Konicki, W., Hełminiak, A., Arabczyk, W., Mijowska, E. (2017). Removal of anionic dyes using magnetic Fe@graphite core-shell nanocomposite as an adsorbent from aqueous solutions. *Journal of colloid and interface science, 497*, 155-164.

[2] Peng, X., Huang, D., Odoom-Wubah, T., Fu, D., Huang, J., Qin, Q. (2014). Adsorption of anionic and cationic dyes on ferromagnetic ordered mesoporous carbon from aqueous solution: Equilibrium, thermodynamic and kinetics. *Journal of Colloid and Interface Science, 430*, 272-282.

[3] Konicki,W., Aleksandrzak, M., Moszyński, D., Mijowska, E. (2017). Adsorption of anionic azo-dyes from aqueous solutions onto graphene oxide: Equilibrium, kinetic and thermodynamic studies. *Journal of colloid and interface science, 496*, 188-200.

[4] Khamparia, S., Jaspal, D. (2016). Adsorptive removal of Direct Red 81 dye from aqueous solution onto argemone mexicana. *Sustainable environment research, 26*(3), 117-123.

[5] Cheng, Z., Zhang, L., Guo, X., Jiang, X., Li, T. (2015). Adsorption behavior of Direct Red 80 and congo red onto activated carbon/surfactant: Process optimization, kinetics and equilibrium. *Spectrochimica acta part A, 137*, 1126-1143.

[6] Qi, Y., Yang, M., Xu, W., He, S., Men, Y. (2017). Natural polysaccharides-modified graphene oxide for adsorption of organic dyes from aqueous solutions. *Journal of colloid and interface science, 486*, 84-96.

[7] Zodi, S., Merzouk, B., Potier, O., Lapicque, F., Leclerc, J. P. (2013). Direct red 81 dye removal by a continuous flow electrocoagulation/ flotation reactor. *Separation and purification technology, 108*, 215-222.

[8] Yang, S., Wang, L., Zhang, X., Yang, W., Song, G. (2015). Enhanced adsorption of Congo red dye by functionalized carbon nanotube/mixed metal oxides nanocomposites derived from layered double hydroxide precursor. *Chemical engineering journal*, *275*, 315-321.

[9] El-Bindary, A. A., Hussien, M. A., Diab, M. A., Eessa, A. M. (2014). Adsorption of Acid Yellow 99 by polyacrylonitrile/activated carbon

composite: Kinetics, thermodynamics and isotherm studies. *Journal of molecular liquids, 197*, 236-242.

[10] El Boujaady, H., Mourabet, M., Bennani-Ziatni, M., Taitai, A. (2014). Adsorption/desorption of Direct Yellow 28 on apatitic phosphate: Mechanism, kinetic and thermodynamic studies. *Journal of the association of Arab universities for basic and applied sciences, 16*, 64-73.

[11] Sharififard, H. (2018). Statistical physics modeling of equilibrium adsorption of cadmium ions onto activated carbon, chitosan and chitosan/activated carbon composite. *Advances in environmental technology, 4*(3), 149-154.

[12] Sharififard, H., Lashanizadegan, A., Pazira, R., Darvishi, P. (2018). Xylene removal from dilute solution by palm kernel activated charcoal: Kinetics and equilibrium analysis. *Advances in environmental technology, 4*(2), 107-117.

[13] Azizi, A., Torabian, A., Moniri, E., Hassani, A. H., Ahmad Panahi, H. (2017). Novel synthesis of graphene oxide with polystyrene for the adsorption of toluene, ethylbenzene and xylenes from wastewater. *Desalination and water treatment, 74*, 248-257.

[14] Azizi, A., Torabian, A., Moniri, E., Hassani, A. H., Ahmad Panahi, H. (2018). Investigating the removal of ethylbenzene from aqueous solutions using modified graphene oxide: Application of response surface methodology. *International journal of environmental science and technology*, *15*(12), 2669-2678.

[15] Rokni, S., Shirazi, R. H. S. M., Miralinaghi, M., Moniri, E. (2020). Efficient adsorption of anionic dyes onto magnetic graphene oxide coated with polyethylenimine: Kinetic, isotherm, and thermodynamic studies. *Research on chemical intermediates, 46*(4), 2247-2274.

[16] De Assis, L. K., Damasceno, B. S., Carvalho, M. N., Oliveira, E. H., Ghislandi, M. G. (2020). Adsorption capacity comparison between graphene oxide and graphene nanoplatelets for the removal of coloured textile dyes from wastewater. *Environmental technology, 41*(18), 2360-2371.

[17] Hummers, W. S., Offeman, R. E. (1958). Preparation of graphitic oxide. *Journal of the American chemical society, 80*(6), 1339.

[18] Azizi, A., Alavi Moghaddam, M. R., Arami, M. (2011). Application of response surface methodology for optimization of reactive blue 19 dye removal from aqueous solutions using pulp and paper sludge. *Fresenius environmental bulletin, 20*(4), 929-938.

[19] Kafshgari, L. A., Ghorbani, M., Azizi, A., Agarwal, S., Gupta, V. K. (2017). Modeling and optimization of Direct Red 16 adsorption from aqueous solutions using nanocomposite of $MnFe_2O_4$/MWCNTs: RSM-CCRD model. *Journal of molecular liquids, 233*, 370-377.

[20] Azizi, A., Alavi Moghaddam, M. R., Arami, M. (2012). Application of wood waste for removal of reactive blue 19 from aqueous solutions: Optimization through response surface methodology. *Environmental engineering and management journal, 11*(4), 795-804.

[21] Ganesan, P., Kamaraj, R., Vasudevan, S. (2013). Application of isotherm, kinetic and thermodynamic models for the adsorption of nitrate ions on graphene from aqueous solution. *Journal of the Taiwan institute of chemical engineers, 44*(5), 808-814.

[22] Sharma, P., Saikia, B. K., Das, M. R. (2014). Removal of methyl green dye molecule from aqueous system using reduced graphene oxide as an efficient adsorbent: Kinetics, isotherm and thermodynamic parameters. *Colloids and surfaces A, 457*, 125-133.

[23] Sadaf, S., Bhatti, H. N., Nausheen, S., Amin, M. (2015). Application of a novel lignocellulosic biomaterial for the removal of Direct Yellow 50 dye from aqueous solution: Batch and column study. *Journal of the Taiwan institute of chemical engineers, 47*, 160-170.

[24] Minitha, C. R., Lalitha, M., Jeyachandran, Y. L., Senthilkumar, L., Rajendra Kumar, R. T. (2017). Adsorption behaviour of reduced graphene oxide towards cationic and anionic dyes: Co-action of electrostatic and π – π interactions. *Materials chemistry and physics, 194*, 243-252.

[25] Ghaedi, M., Sadeghian, B., Pebdani, A. A., Sahraei, R., Daneshfar, A., Duran, C. (2012). Kinetics, thermodynamics and equilibrium

evaluation of direct yellow 12 removal by adsorption onto silver nanoparticles loaded activated carbon. *Chemical engineering journal, 187*, 133-141.

[26] Doulati Ardejani, F., Badii, K., Yousefi Limaee, N., Mahmoodi, N. M., Arami, M., Shafaei, S. Z., Mirhabibi, A. R. (2007). Numerical modelling and laboratory studies on the removal of Direct Red 23 and Direct Red 80 dyes from textile effluents using orange peel, a low-cost adsorbent. *Dyes and pigments, 73*(2), 178-185.

[27] De Jesus da Silveira Neta, J., Costa Moreira, G., Da Silva, C. J., Reis, C., Reis, E. L. (2011). Use of polyurethane foams for the removal of the Direct Red 80 and Reactive Blue 21 dyes in aqueous medium. *Desalination, 281*, 55-60.

[28] Doulati Ardejani, F., Badii, K., Yousefi Limaee, N., Shafaei, S. Z., Mirhabibi, A. R. (2008). Adsorption of Direct Red 80 dye from aqueous solution onto almond shells: Effect of pH, initial concentration and shell type. *Journal of hazardous materials, 151*(2-3), 730-737.

[29] Arami, M., Yousefi Limaee, N., Mahmoodi, N. M., Tabrizi, N. S. (2006). Equilibrium and kinetics studies for the adsorption of direct and acid dyes from aqueous solution by soy meal hull. *Journal of hazardous materials, 135*(1-3), 171-179.

[30] Deng, X., Lü, L., Li, H., Luo, F. (2010). The adsorption properties of Pb(II) and Cd(II) on functionalized graphene prepared by electrolysis method. *Journal of hazardous materials, 183*(1-3), 923-930.

[31] Rajesh, R., Iyer, S. S., Ezhilan, J., Kumar, S. S., & Venkatesan, R. (2016). Graphene oxide supported copper oxide nanoneedles: An efficient hybrid material for removal of toxic azo dyes. *Spectrochimica acta Part A, 166*, 49-55.

[32] Chowdhury, S., Balasubramanian, R. (2014). Recent advances in the use of graphene-family nanoadsorbents for removal of toxic pollutants from wastewater. *Advances in colloid and interface science, 204*, 35-56.